Propagation and Breaking of Nonlinear Kelvin Waves

ALEXEY V. FEDOROV AND W. KENDALL MELVILLE

Scripps Institution of Oceanography, University of California San Diego, La Jolla, California

(Manuscript received 19 April 1994, in final form 9 December 1994)

ABSTRACT

The evolution of nonlinear Kelvin waves is studied using analytical and numerical methods. In the absence of dispersive (nonhydrostatic) effects, such waves may evolve to breaking. The authors find that one of the effects of rotation is to delay the onset of breaking in time by up to 60%, with respect to a comparable wave in the absence of rotation. This delay is consistent with qualitative conclusions based on transverse averaging of the evolution equations. Further, the onset of breaking occurs almost simultaneously over a zone of uniform phase that is normal to the boundary and extends over a distance comparable to the Rossby radius of deformation. In other words, the process of breaking embraces the most energetic area of the wave. In contrast to the linear Kelvin wave, the nonlinear wave develops a dipole structure in the cross-shelf velocity, with a zero net offshore flow. With increasing nonlinearity the flow develops a stronger offshore jet ahead of the wave crest. The Kelvin wave amplitude at the coast decays slightly with time. This and other major features of the wave are accounted for by an analytical model based on slowly varying averaged variables. As part of the analysis it is demonstrated that the evolution of the wave phase may be described by an inhomogeneous Klein–Gordon equation.

1. Introduction

Internal Kelvin waves play a significant role in the dynamics of the coastal oceans. In recent years a considerable amount of work has been done in both experimental and theoretical research on the nonlinear aspects of the Kelvin wave evolution. Most of the theoretical work has been within the framework of KdV-type (Grimshaw 1985; Melville et al. 1989, 1990; Grimshaw and Melville 1989) or Boussinesq-type equations (Tomasson and Melville 1992). These equations may include three-dimensional and rotational effects, together with dispersive (nonhydrostatic) effects (Tomasson and Melville 1990; Tomasson 1991; also see appendix A of this paper). Regardless of the particular approach, an important assumption of these studies, as well as laboratory experiments (Renouard et al. 1992), was that the dispersion and nonlinearity were of the same order. This assumption led to an approximate balance between nonlinearity and dispersion. However, in many physical situations involving long waves, the dispersion is weak and waves may behave in a typical nonlinear hyperbolic manner leading to wave breaking (Whitham 1974; Boyd 1980). For instance, an estimate of the parameters for a coastal internal Kelvin wave of about 5-km wavelength and 1.5-h period corresponding to a 10-km Rossby radius of deformation shows that the dispersion effects may be four orders of magnitude weaker than the nonlinear effects (appendix A). In turn, breaking of the internal waves may be important in mixing and momentum and energy transfer in coastal oceans.

A similar situation may arise during the propagation of atmospheric internal bores (Marks 1974; Smith et al. 1982) with three-dimensional wave evolution influenced by nonlinearity and rotation. Dorman (1985) investigated the possibility of atmospheric Kelvin waves propagating in the low marine layer adjacent to the coast of California. Similar phenomena were observed along the coast of Australia (Baines 1980) and southern Africa (Gill 1977; Bannon 1981). To study these cases we start with the shallow-water equations for a single-layer fluid:

$$u_t + uu_x + vu_y + gh_x - fv = 0, \quad (1.1a)$$

$$v_t + uv_x + vv_y + gh_y + fu = 0, \quad (1.1b)$$

$$h_t + (uh)_x + (vh)_y = 0. \quad (1.1c)$$

The notation is conventional (Pedlosky 1987, 61), with $h(x, y, t)$ denoting the entire local height of the layer, $u(x, y, t)$ the alongshore velocity, $v(x, y, t)$ the offshore velocity, and g the effective gravity. Then following a standard approach we introduce nondimensional variables

$$u = \alpha c u', \quad (1.2)$$

$$v = \alpha\gamma^{1/2} c v', \quad (1.3)$$

$$h = H(1 + \alpha\eta), \quad (1.4)$$

$$x = L_x x', \quad (1.5)$$

Corresponding author address: Dr. W. Kendall Melville, Scripps Institution of Oceanography, University of California, San Diego, La Jolla, CA 92093-0230.

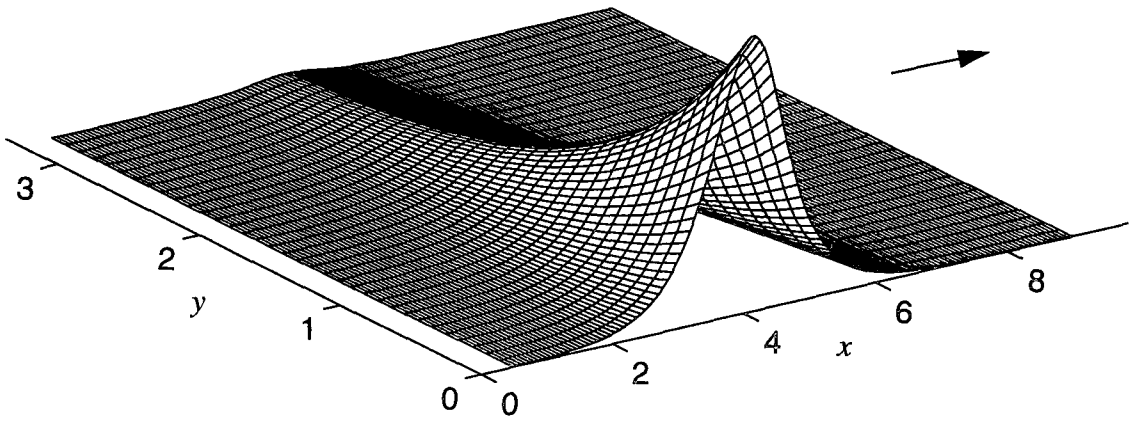

FIG. 1. Propagation of a localized Kelvin wave along the coast. The graph shows the elevation of the interface η at the initial time. The wave is traveling to the right.

$$y = \mathrm{Ro}\, y', \tag{1.6}$$

$$t = \frac{L_x}{c} t', \tag{1.7}$$

where

$$\alpha = \frac{h}{H}, \tag{1.8}$$

$$\gamma = \left(\frac{L_x}{\mathrm{Ro}}\right)^2, \tag{1.9}$$

$$c = (gH)^{1/2}, \tag{1.10}$$

and

$$\mathrm{Ro} = \frac{c}{f}. \tag{1.11}$$

Here h is a typical wave amplitude, L_x is a typical wavelength, H is the layer depth (equivalent height in two-layer models), and Ro is the Rossby radius of deformation. We consider the case when α and γ are much smaller than unity and $\gamma = O(\alpha)$. Substituting (1.2) through (1.11) into (1.1) and dropping the primes gives

$$u_t + \eta_x + \alpha u u_x - \gamma v = O(\alpha\gamma), \tag{1.12a}$$

$$\gamma(v_t + \eta_y + u) = O(\alpha\gamma), \tag{1.12b}$$

$$\eta_t + u_x + \gamma v_y + \alpha(u\eta)_x = O(\alpha\gamma). \tag{1.12c}$$

For the wave moving to the right, Eqs. (1.12a) and (1.12c) yield

$$\eta = u + O(\alpha) \tag{1.13}$$

and

$$\eta_t + \eta_x = O(\alpha). \tag{1.14}$$

Further, following Whitham (1974) and matching the asymptotic expansions from (1.12a), (1.12c), and (1.13) we obtain

$$\eta_t + \eta_x + \frac{3}{2}\alpha\eta\eta_x + \frac{\gamma}{2}(v_y - v) = O(\alpha\gamma). \tag{1.15}$$

Equations (1.12b) and (1.15), together with (1.13), describe nonlinear wave propagation with weak transverse and rotational effects, which is the subject of this paper:

$$\eta_t + \eta_x + \frac{3}{2}\alpha\eta\eta_x + \frac{\gamma}{2}(v_y - v) = 0 \tag{1.16}$$

$$v_t + \eta_y + \eta = 0. \tag{1.17}$$

Full derivations of such coupled evolution equations for one- and two-layer models, including dispersion effects, are given in several papers (Macomb 1986; Grimshaw and Melville 1989; Tomasson 1991). The nonlinear term proportional α in (1.16) is due to both momentum and mass conservation equations [cf. Hua and Thomasset (1983), who considered only nonlinearity from the momentum equation]. The term proportional to γ describes weak rotation and the effect of weak offshore flow.

We study the evolution of an initial localized disturbance (Fig. 1) in a semi-infinite ocean subject to a no-flux condition at the boundary:

$$\eta|_{t=0} = e^{-y}\Phi(x), \quad v|_{t=0} = 0 \tag{1.18}$$

$$v|_{y=0} = 0, \tag{1.19}$$

with the initial condition corresponding to a linear Kelvin wave. Despite the seemingly simple character of the system, it has a number of interesting physical properties.

A similar initial value problem was studied by Melville et al. (1989) with two main differences:

1) dispersion was comparable to nonlinearity and was explicitly included in (1.16)—see appendix A;

2) the waves propagated in a relatively narrow channel.

The instability and damping of solitary-type Kelvin waves due to the radiation of Poincare waves was observed. In the present study we do not observe any significant Poincare wave radiation up to breaking. The main difference is that now the equations belong to the hyperbolic, rather than dispersive, class of equations. This implies that multivalue profiles may arise, resulting in a typical hyperbolic wave breaking.

One of the first attempts to study nonlinear nondispersive Kelvin waves was undertaken by Bennet (1973). He dealt with freely propagating nonlinear Kelvin waves with a wavelength larger than the Rossby radius of deformation. In our work we consider waves with a wavelength smaller than the Rossby radius (see appendix A). Also, Bennet assumed that the transverse balance of the velocity was geostrophic, which is equivalent to dropping the term v_t in (1.2). Our conclusion is that the cumulative effect of even small offshore velocities significantly affects the wave steepening and, ultimately, breaking.

We show that the onset of breaking is delayed by up to 60% in time with respect to a comparable long wave in the absence of rotation. Breaking occurs almost simultaneously in a region adjacent to the coast having a width comparable to the Rossby radius of deformation. If $\max|\Phi_x| = 1$, the time of breaking can still be calculated as c/α, c being a constant between 1 and 2 with a parametric dependence on γ. The transverse velocity itself forms a dipole structure attached to the wave.

Also we show that the original nonlinear problem can be reduced to a forced linear Klein–Gordon equation. The Klein–Gordon equation describes the evolution of the wave phase, which gives the location of the wave crest and time of breaking.

2. Preliminary considerations

We first undertake a qualitative examination of Eqs. (1.16)–(1.17) to demonstrate some features of the wave evolution. Transforming to a frame of reference moving with the linear phase speed to the right and renormalizing α and γ gives

$$\eta_t + \alpha\eta\eta_x + \gamma(v_y - v) = 0, \tag{2.1}$$

$$v_t - v_x + \eta_y + \eta = 0. \tag{2.2}$$

If one neglects the nonlinear term, setting $\alpha = 0$, then the solution of (2.1) and (2.2) is

$$\eta = e^{-y}\Phi(x), \tag{2.3}$$

where $\Phi(x)$ is an arbitrary function. This describes a linear Kelvin wave. When $\alpha \neq 0$, integrating with respect to y and using the boundary conditions gives

$$\left(\frac{\partial}{\partial t} - \frac{\partial}{\partial x}\right)(\overline{\eta}_t + \alpha\overline{\eta\eta_x}) = \gamma(\eta|_{y=0} - \overline{\eta}), \tag{2.4}$$

where

$$\overline{\eta} = \int_0^\infty \eta dy. \tag{2.5}$$

If one assumes that to the leading order the wave is still a Kelvin wave, that is,

$$\eta = e^{-y}F(x, t, y) + O(\alpha) \tag{2.6}$$

and

$$\frac{\partial F}{\partial y} = O(\alpha), \tag{2.7}$$

then (2.4) reduces to

$$\overline{\eta}_t + \frac{\alpha}{2}\overline{\eta}\overline{\eta}_x = O(\alpha^2). \tag{2.8}$$

It follows from (2.8) that the onset of breaking may begin at $t < 2/\alpha$ (see section 3 below). That is, the Kelvin wave may propagate without breaking for up to twice the time of a nonlinear wave in the absence of rotation.

In addition, there exist several conservation integrals for the system. Introducing x-integrated variables,

$$\tilde{\eta} = \int_{-\infty}^{\infty} \eta dx \quad \text{and} \quad \tilde{v} = \int_{-\infty}^{\infty} v dx, \tag{2.9}$$

(2.1) and (2.2) give

$$\tilde{\eta}_{tt} + \gamma(\tilde{\eta} - \tilde{\eta}_{yy}) = 0 \tag{2.10}$$

and

$$\tilde{v}_{tt} + \gamma(\tilde{v} - \tilde{v}_{yy}) = 0. \tag{2.11}$$

Further, for the initial profile (1.3) there are mass conservation integrals:

$$\tilde{\eta} = \int_{-\infty}^{\infty} \eta dx = \tilde{c}e^{-y}, \tag{2.12}$$

where

$$\tilde{c} = \int_{-\infty}^{\infty} \Phi dx, \tag{2.13}$$

and

$$\tilde{v} = \int_{-\infty}^{\infty} v dx = 0. \tag{2.14}$$

The second integral shows that there is no net cross-shelf flow for the nonlinear Kelvin wave. Zero net offshore flow appears to be a typical feature of freely propagating Kelvin waves (see section 5).

Finally, there are two more integrals:

$$\int_{-\infty}^{\infty}\int_{0}^{\infty}(\eta^2 + \gamma v^2)dxdy = \text{const} \qquad (2.15)$$

and

$$\int_{-\infty}^{\infty}\int_{0}^{\infty}\left(\frac{\alpha}{6}\eta^3 + \gamma v(\varphi + \varphi_y - v/2)\right)dxdy = \text{const}, \qquad (2.16)$$

with

$$\eta = \varphi_x. \qquad (2.17)$$

The last integral expresses the conservation of the Hamiltonian for the system. With the addition of dispersion effects, all the integral constraints persist, except for expression (2.14) that gains an extra term.

3. Numerical results

The numerical scheme used for solving the system (1.1)–(1.2) is simple and rather stable. It is an implicit staggered-mesh scheme, similar to that described by Melville et al. (1989) and Tomasson (1991), with centered differences for spatial derivatives. Similar staggered-mesh grids for linear Kelvin waves were presented by Hsieh et al. (1983) and for nonlinear forced disturbances by Hua and Thomasset (1983), to name a few. The scheme, which we used, had second-order accuracy in space and time. The consistency and reliability of the scheme was tested by switching off one of the parameters α or γ. In both cases a comparison with available analytical solutions confirmed the accuracy of the numerical approach. An example of this verification will be demonstrated below. Four main combinations of parameters α and γ were studied: (α, γ) = (0.5, 0.5), (0.5, 0.125), (0.125, 0.125), (0.125, 0.5). For the sake of clarity of the discussion, we will present detailed results for (0.5, 0.5) and then outline the effect of changing α and γ.

The initial profile chosen was

$$\Phi(x) = \frac{1}{\cosh(2x)}, \qquad (3.1)$$

with $|\Phi_x| \leq 1$, which will be important for the construction of the analytical model.

The main question, which arose in the numerical treatment, was how to define the moment of breaking for the wave. As long as we do not introduce any additional terms in the system, the only possible breaking would be numerical, as profiles develop gradients beyond the stability limits of the numerical scheme. Further, we anticipate that in reality the wave will evolve to breaking if its steepness exceeds a certain threshold. We expect that numerical breaking will be a good indicator of physical breaking if the spatial resolution of the numerical scheme is sufficiently high.

The second question to resolve was how to recognize the onset of breaking itself; that is, how to distinguish between the breaking and small short-wavelength oscillations, which appeared sometimes on the forward face of the wave. Considering breaking as a global phenomenon rather than a local event, we attributed the onset of breaking to the moment that all the pertinent parameters of the wave experienced a substantial change. As an example, Fig. 2 demonstrates such a change of the behavior of the wave amplitude at the coast at time $t \approx 3.0$. For comparison we also present the graph for the evolution of the amplitude in the absence of rotation (dashed line), which is obtained from the same numerical scheme but without rotational terms. In the absence of rotation, the time of breaking may be calculated from a well-known analytical result that $t_{\text{breaking}} = 1/\alpha$ [see Whitham (1974) and section 4 of this paper], which is in complete agreement with the numerical result. Thus, from the figure we can see that the rotational effect is to delay the onset of breaking by 50% (from $t = 2$ to $t = 3$) and to slightly decrease the wave amplitude as well. To demonstrate the global character of the breaking, in Fig. 2 we show the graphs for the evolution of other wave parameters, including the wave amplitude at $y = 0.5$ and the maximum transverse velocity in the wave.

Note that a decay in the amplitude of the nonlinear Kelvin waves has been reported by various authors. They attributed the decay to the secondary wave radiation excited by the Kelvin wave (Maxworthy 1983;

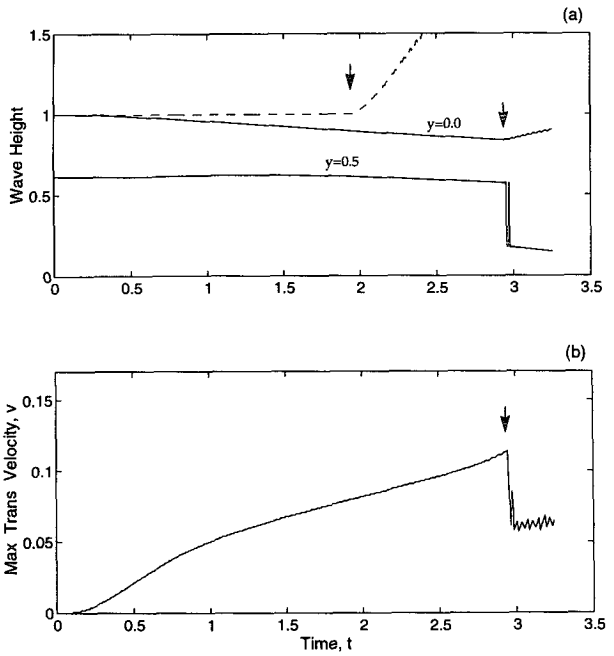

FIG. 2. (a) The amplitude of a Kelvin wave vs time (solid line) at the coastline and away from the coast ($y = 0$, $y = 0.5$) from numerical calculations. The onset of breaking is shown by arrows. The amplitude of the wave in the absence of rotation is given by the dashed line; $\alpha = 0.5$, $\gamma = 0.5$. (b) The evolution of the maximum value of the transverse velocity in the wave.

Melville et al. 1989) or viscosity (Renouard et al. 1987). In our system the combined transverse–rotational term plays a similar role to dispersion, causing an increase in the characteristic length of the wave and a consequent decrease in the wave amplitude. However, this dispersion is not sufficient to balance the nonlinearity and to lead to solitary-like waves (cf. Katsis et al. 1987; Melville et al. 1989; Renouard et al. 1992). Here the Kelvin wave steepens and then breaks.

Now to give a general overview of the wave evolution, we present contour maps for the elevation of the interface η and the transverse velocity v for different times (see Fig. 3). There are several important points worth mentioning here, including the formation of a dipole structure in the transverse velocity associated with the wave and the general curvature of the wave front due to nonlinearity. Also, notice the compression of the isolines ahead of the wave corresponding to the increasing steepness of the wave. This conforms to the typical hyperbolic character of the breaking.

The next interesting feature of the wave is the formation of a boundary zone adjacent to the coast, which we call a uniform phase zone. This zone is clearly shown by the plots of

1) the wave height along the wave crest and
2) the wave height versus distance offshore

for different times (Fig. 4). We find that for some distance from the coast the two plots coincide exactly (see the figure), which means that the crest of the wave remains normal to the wall over the entire zone or, equivalently, the phase of the wave is constant. The width of the boundary zone increases with time and eventually extends to distances comparable to the Rossby radius of deformation, which is of the order of one in our nondimensional variables. Breaking takes place almost simultaneously over the whole region and therefore covers the most energetic part of the wave. Also in contrast to previous studies (Katsis and Akylas 1987; Melville et al. 1989) and despite the general distortion of the wave front due to nonlinearity, the curvature remains zero in the boundary zone.

In Fig. 5 we show a profile of the transverse velocity at a time just before breaking for $y = 0.1$ and $y = 0.5$. A relatively sharp and strong jet has formed ahead the wave. Although the values of the transverse velocity are still very low (not more than 0.2), over long times it leads to a significant change in the wave evolution.

To summarize the results for different α and γ we present some pertinent wave parameters in Table 1.

4. Analytical model

We now consider a simple model that embraces all the significant features of the evolution found in the numerical solutions. As the basis for the model we assume that to the leading order the solution is a Kelvin wave with almost exponentially decaying amplitude.

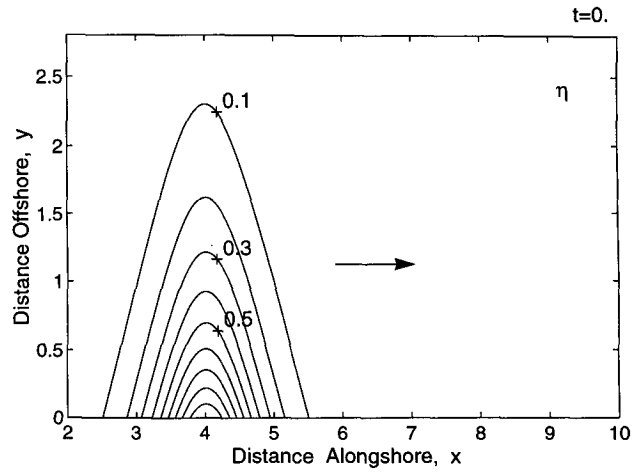

FIG. 3a. Contour map for the elevation of the interface η at the initial time ($t = 0$).

We also expect that any breaking will be similar to regular breaking of long gravity waves (hyperbolic breaking). The elevation of the interface η is assumed to take the form

$$\eta = ae^{-y}\hat{\eta}, \tag{4.1}$$

where

$$\hat{\eta} = \Phi(ax - \Theta\hat{\eta}), \tag{4.1a}$$

with both a and Θ depending upon t and y. Notice that η given by expression (4.1) obeys the mass conservation equation [see (2.11)] and is a generalization of a well-known implicit solution $\eta = \Phi(x - \alpha t\eta)$ for the equation

$$\eta_t + \alpha\eta\eta_x = 0, \tag{4.2}$$

(see Whitham 1974; Boyd 1980).

From (4.1)

$$\eta_x = \frac{a^2 e^{-y}\Phi_\xi}{1 + \Theta\Phi_\xi}, \tag{4.3}$$

where

$$\Phi = \Phi(\xi) \tag{4.4}$$

and

$$\xi = ax - \Theta\hat{\eta}. \tag{4.4a}$$

Breaking occurs when the steepness of the wave becomes infinite; that is,

$$1 + \Theta\Phi_\xi = 0 \quad \text{or} \quad \Theta = -\frac{1}{\Phi_\xi}. \tag{4.5}$$

Thus, breaking occurs when $\Theta = \Theta_{\text{breaking}} = 1$ (since $\max|\Phi_\xi| = 1$), after which the model is no longer valid.

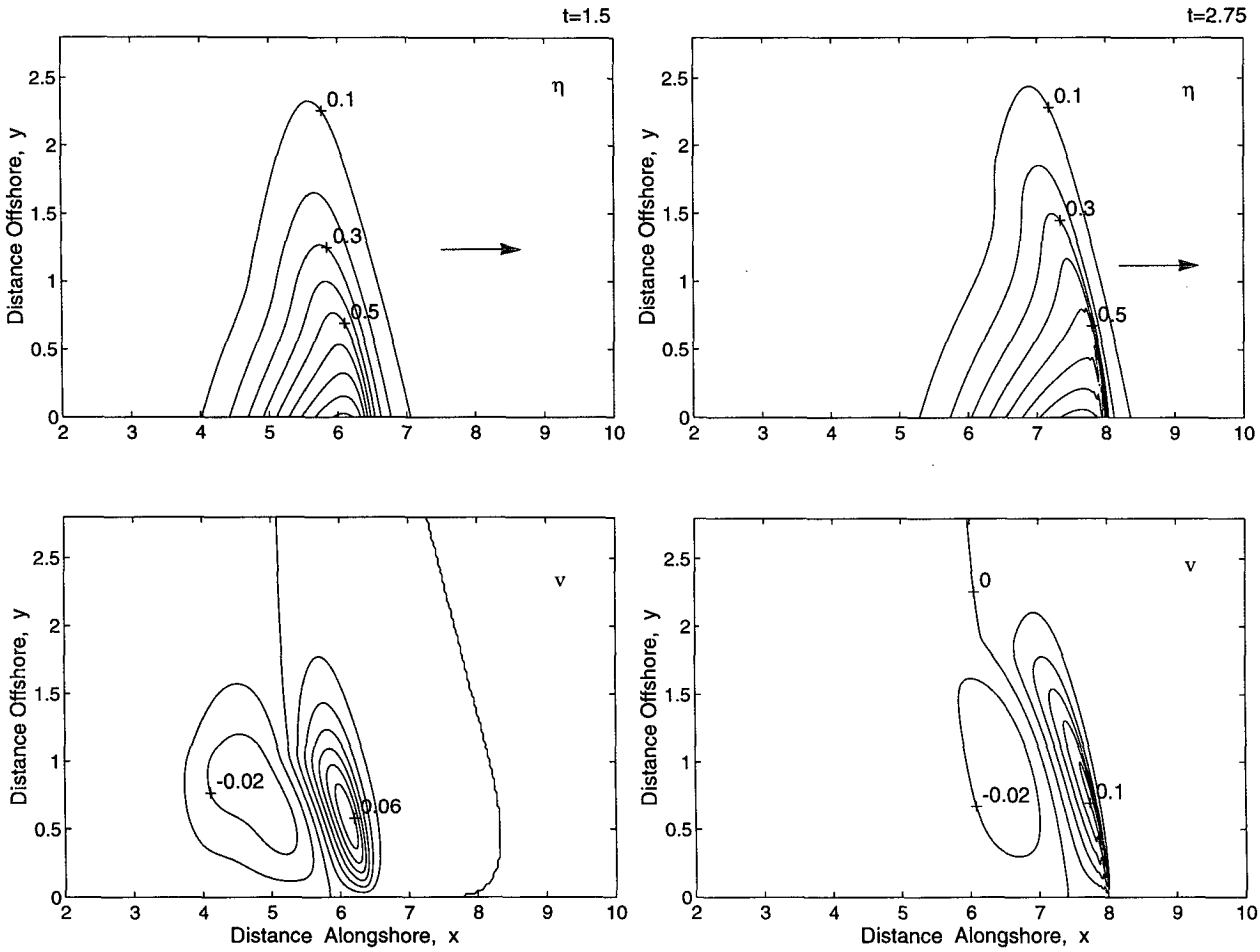

FIG. 3 (*Continued*) Direct numerical solution giving contour maps of the elevation of the interface η and transverse velocity v at $t = 1.5$ and $t = 2.75$ for $\alpha = 0.5$, $\gamma = 0.5$. Breaking occurs at $t = 3.0$.

On the other hand, the profile of the wave crest is determined by condition $\eta_x = 0$. This implies that the x coordinate of the wave crest is $\Theta_c = \Theta_{\text{crest}} = \Theta/a$. Thus, we can call Θ_c the wave phase. As long as $a \approx 1$, $\Theta_c \approx \Theta$. Further, from (4.1)–(4.4) it can be shown that

$$\eta\eta_x = a^2 e^{-2y}\Phi\Phi_x, \tag{4.6a}$$

$$\eta_t = \frac{a_t}{a} e^{-y}(\Phi\xi)_x + \left(-\Theta_t + 2\Theta\frac{a_t}{a}\right)e^{-y}\Phi\Phi_x, \tag{4.6b}$$

$$\eta + \eta_y = \frac{a_y}{a} e^{-y}(\Phi\xi)_x + \left(-\Theta_y + 2\Theta\frac{a_y}{a}\right)e^{-y}\Phi\Phi_x. \tag{4.6c}$$

This prompts us to search for an approximate solution for the transverse velocity v in the form

$$v = be^{-y}\Phi\Phi_x + de^{-y}(\Phi\xi)_x, \tag{4.7}$$

where

$$b = b(t, y) \quad \text{and} \quad d = d(t, y). \tag{4.8}$$

We will satisfy the original equations in an average sense (see below) to obtain a description of the evolution of the wave amplitudes and phase. Note that (4.7) is consistent with the zero net transverse flow condition, and it appears to be a good approximation for v, at least for short periods of time.

We seek the relationships between a, b, d, Θ under the following constraints:

$$a = 1 + O(\alpha), \tag{4.9a}$$

$$b, d, a_y, a_t, \Theta_y, \Theta_t \leqslant O(\alpha), \tag{4.9b}$$

and

$$\Theta < 1. \tag{4.9c}$$

Substituting expressions (4.6)–(4.8) into the basic equations (2.1)–(2.2) yields

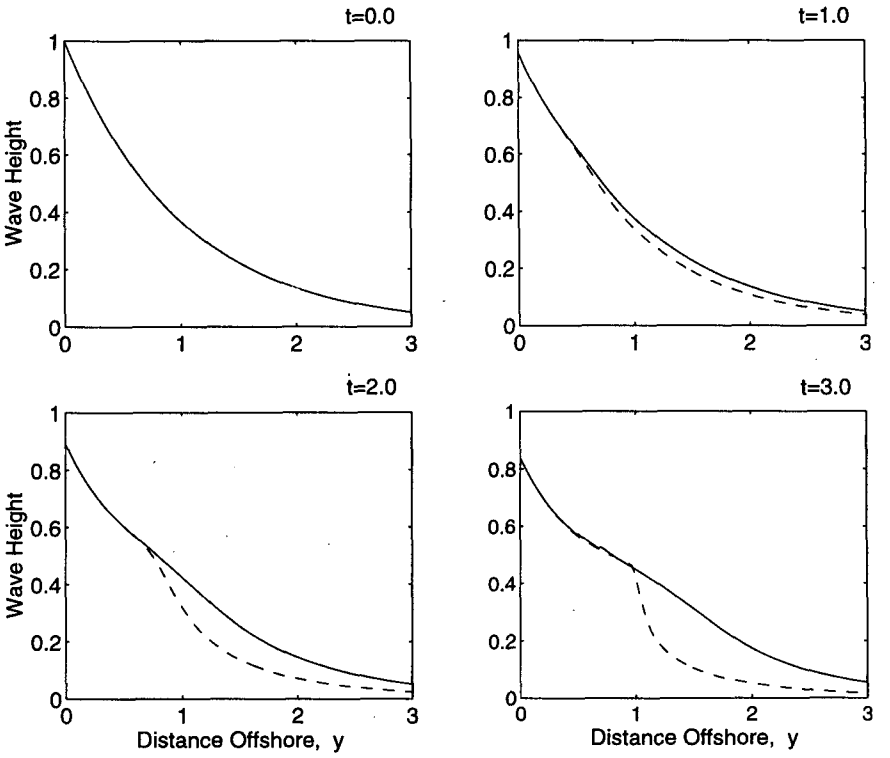

FIG. 4. Evidence for the uniform phase zone: the wave height along the wave crest—solid line, the wave height vs distance offshore—dashed line; for $\alpha = 0.5$, $\gamma = 0.5$.

$$\left(-\Theta_t + 2\Theta\frac{a_t}{a} + \alpha a^2 e^{-y}\right)\frac{\Phi^2}{2} + \frac{a_t}{a}\Phi\xi = \gamma(2b - b_y)\frac{\Phi^2}{2} + \gamma(2d - d_y)\Phi\xi, \quad (4.10a)$$

$$b_t\frac{\Phi^2}{2} + d_t\Phi\xi - b\Phi\Phi_x - d(\Phi\xi)_x + \frac{a_y}{a}\Phi\xi - \left(\Theta_y - 2\Theta\frac{a_y}{a}\right)\frac{\Phi^2}{2} = 0, \quad (4.10b)$$

with the nonlinear terms proportional to $\gamma\Theta_y b$, $\gamma\Theta_y d$ in (4.10a) and to $\Theta_t b$, $\Theta_t d$ in (4.10b) omitted. Eventually all of them would give a correction of $O(\gamma\alpha^2)$.

Now we can obtain weighted integrals of (4.10a) and (4.10b) with respect to x, using Φ^m and $\Phi^{m-1}\xi$ (m positive) as weighting functions to give

$$\left(\Theta_t - 2\Theta\frac{a_t}{a}\right) + \gamma(2b - b_y) = \alpha a^2 e^{-y} \quad (4.11a)$$

$$-\frac{a_t}{a} + \gamma(2d - d_y) = 0 \quad (4.11b)$$

$$b_t - \left(\Theta_y - 2\Theta\frac{a_y}{a}\right) - rd = 0 \quad (4.11c)$$

$$d_t + \frac{a_y}{a} + qb = 0. \quad (4.11d)$$

Another way to arrive at a similar system, based on a nontraditional use of the averaged-Lagrangian formalism, is given in appendix B. Also note that (4.11a) and (4.11b) ensure that (4.10a) is satisfied exactly. The general formulas for r, q are

$$r = r(m) = \frac{2m}{m+1}\cdot\frac{\int_{-\infty}^{\infty}\Phi^{m+1}d\xi}{\int_{-\infty}^{\infty}\Phi^{m+2}d\xi};$$

$$q = q(m) = \frac{1}{m+1}\cdot\frac{\int_{-\infty}^{\infty}\Phi^{m+1}d\xi}{\int_{-\infty}^{\infty}\Phi^{m}\xi^2 d\xi}, \quad (4.12)$$

and their behavior versus m is presented in Fig. 6 for our particular choice of $\Phi(\xi)$ [see (3.1)]. For a reasonable range of m, r and q do not exceed 2–2.5. The system (4.11) reduces to

$$A_t + \frac{\gamma}{a^2}(2B - B_y) = \alpha e^{-y} \quad (4.13a)$$

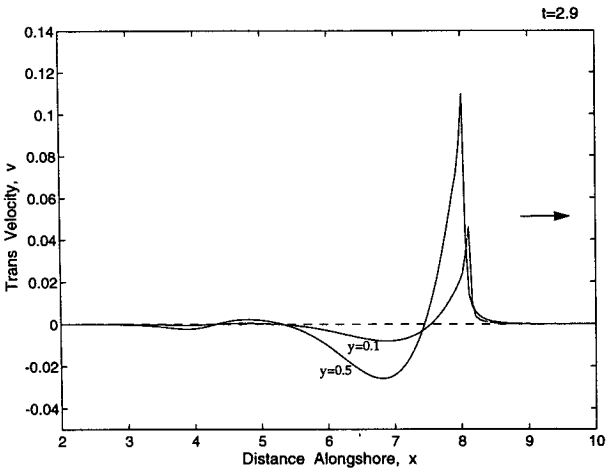

FIG. 5. The profiles of the transverse velocity at the time close to breaking, for two distances offshore ($y = 0.1$, $y = 0.5$). The wave is moving to the right. Positive values of the velocity correspond to offshore flow, negative to onshore flow. The sharp peak (jetlike flow) is caused by the increasing steepness of the wave; for $\alpha = 0.5$, $\gamma = 0.5$.

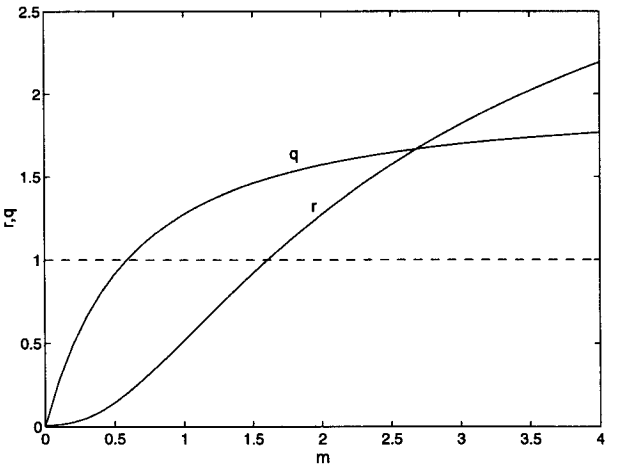

FIG. 6. The behavior of parameters r and q vs m [see Eq. (4.12)].

$$A_y = \frac{1}{a^2}(B_t + ikB), \tag{4.13b}$$

where

$$A = \frac{\Theta + is}{a^2} - is \quad \text{and} \quad B = b + isd, \tag{4.14}$$

$$k = (rq)^{1/2} \quad \text{and} \quad s = \left(\frac{r}{q}\right)^{1/2}, \tag{4.15}$$

with the boundary and initial conditions

$$A = 0|_{t=0};\ B = 0|_{t=0} \tag{4.16a}$$

and

$$A_y = B = 0|_{y=0}. \tag{4.16b}$$

With errors of $O(\gamma\alpha^2)$, Eqs. (4.13) reduce to a single equation:

$$A_{tt} + ikA_t + \gamma(2A_y - A_{yy}) = ik\alpha e^{-y}, \tag{4.17}$$

with

$$A|_{t=0} = 0, \tag{4.17a}$$

$$A_t|_{t=0} = \alpha e^{-y}, \tag{4.17b}$$

and

$$A_y|_{y=0} = 0. \tag{4.17c}$$

Introducing

$$\chi = Ae^{i(k/2)t-y} \quad \text{and} \quad \sigma = \left(\gamma + \frac{k^2}{2}\right)^{1/2} \tag{4.18}$$

leads to the inhomogeneous Klein–Gordon equation

$$\chi_{tt} - \gamma\chi_{yy} + \sigma^2\chi = i\alpha k e^{i(k/2)t-2y}, \tag{4.19}$$

with

$$\chi|_{t=0} = 0, \tag{4.19a}$$

$$\chi_t|_{t=0} = \alpha, \tag{4.19b}$$

TABLE 1.

	α = 0.5	0.5	0.125	0.125
	γ = 0.5	0.125	0.125	0.5
Time of wave breaking	2.95	2.4	11.9	13.0
Time of breaking in the absence of rotation	2.0	2.0	8.0	8.0
Delay of breaking (ratio of the two above)	1.48	1.20	1.49	1.63
Maximum width of the uniform phase zone	0.9	0.3	1.1	1.8
Maximum transverse velocity	0.12	0.18	0.13	0.05

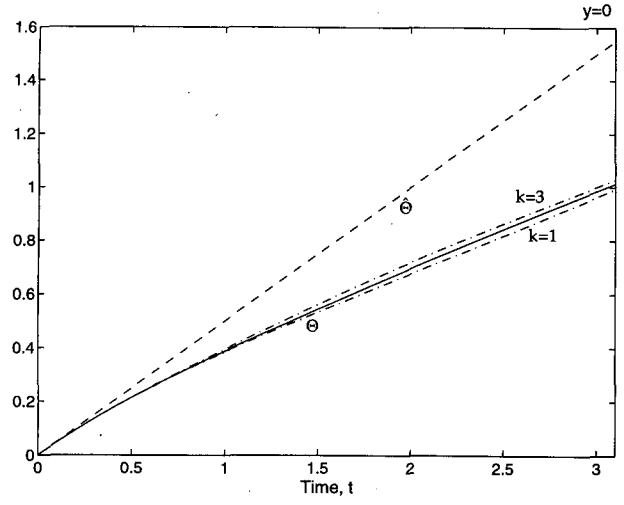

FIG. 7. The evolution of Θ at the coast for different k; $k = 2$—solid line; $k = 1, 3$—dot-dashed lines; for $s = 2.5$. The phase in the absence of rotation $\hat{\Theta} = \alpha t$ is given by the dashed line.

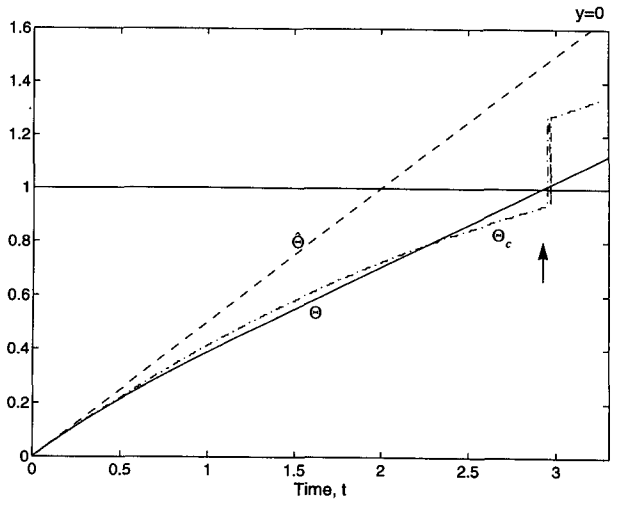

FIG. 8. The evolution of Θ and Θ_c at the coast ($y = 0$). The moment when Θ reaches unity corresponds to breaking. The solid line denotes the value of Θ at the wall; the dashed line the phase in the absence of rotation $\hat{\Theta} = \alpha t$; and the dot-dashed line the phase of the wave Θ_c (location of the crest) from direct numerical calculations. The break in the dot-dashed line is due to numerical breaking; for $\alpha = 0.5$, $\gamma = 0.5$.

$$(\chi + \chi_y)|_{y=0} = 0. \qquad (4.19c)$$

In principle, we can find an explicit solution for (4.17) or (4.19) in terms of Bessel and exponential functions; however, the easiest way is just to numerically invert the Laplace transforms for A or χ obtained from (4.17) or (4.19). Note that formally the term in (4.17) proportional to γ is $O(\alpha\gamma)$, but we have to retain it to satisfy the boundary condition. It can also be shown that if one considers higher-order terms in the derivation in section 1 and then applies the preceding methods, an additional $O(\alpha^2)$ forcing term is obtained on the right-hand side of (4.17). This does not change the essential properties of the system.

The question of the particular choice of k and s remains open. Fortunately, all the parameters proved to be relatively insensitive to changes of k (as an example, see Fig. 7 for the evolution of Θ for different k for $s = 2.5$). The variable b proved to be independent of s, and Θ and a are relatively insensitive to changes of s provided s is not very close to zero. While d depends upon s to a greater degree, its qualitative behavior does not change with s. In general, the qualitative behavior of the model solution does not change over a wide range of values of k and s. Good quantitative agreement with direct numerical calculations is achieved for $k = 2$ and $s = 2.5$. These values are used in presenting the results below.

As we have already pointed out, the phase $\Theta_c = \Theta/a$ determines the shape and location of the crest, while Θ itself determines the time of breaking. In Fig. 8 we again demonstrate the evolution of Θ at the coastline ($y = 0$) for $\alpha = 0.5$, $\gamma = 0.5$, along with the phase in the absence of rotation ($\hat{\Theta} = \alpha t$) and the phase obtained from direct numerical calculations. This comparison shows that the Kelvin wave moves slower, delaying the onset of breaking in time by up to 50%, as obtained from the direct numerical calculations. Only when $\alpha = 0.5$, $\gamma = 0.125$ was the delay less than 30% (20% from the direct numerical calculations). This qualitatively confirms our previous numerical results.

Now consider the y-dependence of the phase Θ_c at the time of breaking. Again for comparison we present the phase of a nonlinear wave for which the speed is just proportional to the amplitude ($\hat{\Theta} = \alpha t e^{-y}$). One can clearly see the appearance of a uniform phase zone

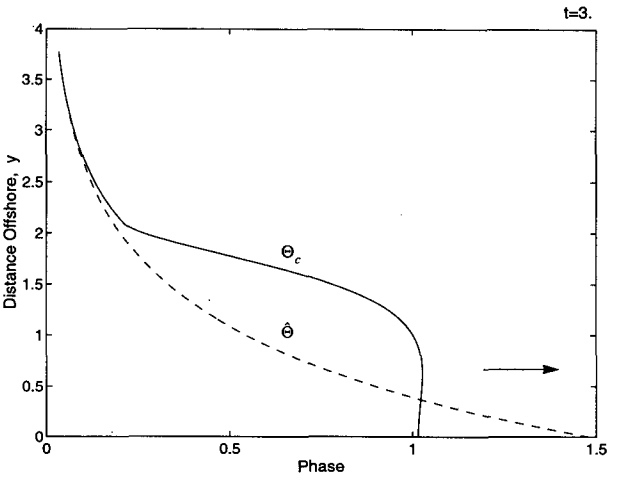

FIG. 9. Prediction of the profile of the phase Θ_c at the moment of breaking (solid line) by the analytical model; $\hat{\Theta} = \alpha t e^{-y}$—dashed line. The arrow indicates the direction of the wave motion; for $\alpha = 0.5$, $\gamma = 0.5$.

(where phase is almost constant; Fig. 9). In most cases it extends to the distances of the order of one in our nondimensional variables. Only for the case $\alpha = 0.5$, $\gamma = 0.125$ did γ appear to be too small and the time necessary for the onset of breaking too short to clearly establish the boundary zone of uniform phase. In general, the width of the zone increases as γ increases. In other words, stronger rotation gives rise to greater boundary influence on the wave. The process of breaking should occur almost simultaneously over the uniform phase zone.

In Fig. 10, we show the model results for the decay of the amplitude at the coastline, together with that from direct numerical calculations, and the evolution of the transverse velocity amplitudes b and d at $y = 0.5$. The model gives a decay of the amplitude at the coastline but fails to predict the exact rate of decay. Next, Fig. 11 shows the contours for η and v obtained from the model (cf., Fig. 3) at time $t = 2$. Only close to the time of breaking does the deviation of the transverse velocity from the direct numerical calculations become visible, a result of limitations in our modeling for v. The dipole structure of the transverse velocity is clearly seen and contours of the elevation of the free surface give a good qualitative description of the wave. Despite some good quantitative agreement, overall the analytical model gives only a qualitative description of the phenomena.

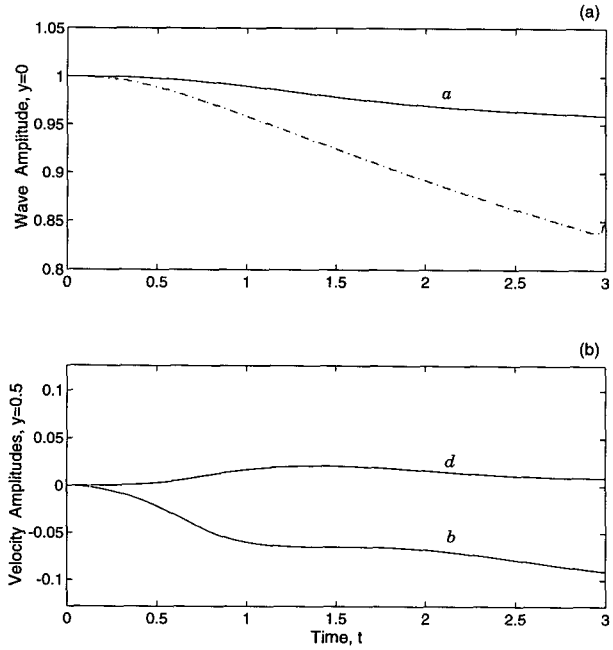

FIG. 10. (a) The wave amplitude evolution at the coast ($y = 0$) from the analytical model (solid line) and from direct numerical calculations (dot-dashed line). (b) The evolution of the transverse velocity amplitudes b and d at $y = 0.5$ from the analytical model; for $\alpha = 0.5$, $\gamma = 0.5$.

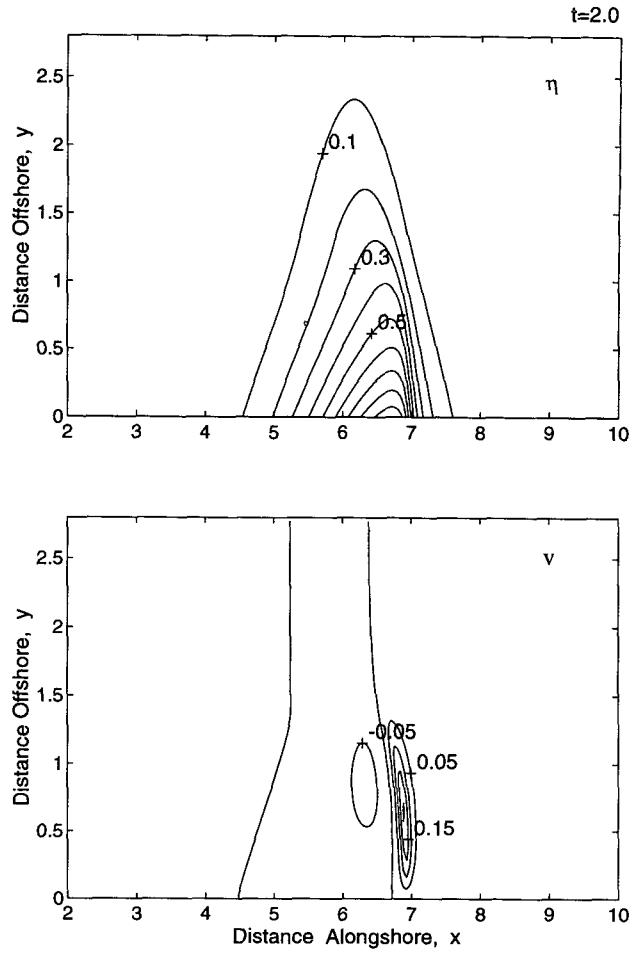

FIG. 11. Contour maps for the elevation of the free surface η and transverse velocity v at time $t = 2$ for $\alpha = 0.5$, $\gamma = 0.5$ from the analytical model (cf. Fig. 3). Breaking occurs at $t = 3$.

Finally, all the conclusions of this section based on the use of the model hold for any choice of the initial function $\Phi(x)$, provided the initial disturbance is localized and symmetric and its characteristic length is of the order of 1. Therefore, our results are quite general in describing the qualitative features of nonlinear nondispersive Kelvin wave evolution.

5. An arbitrary slope of the initial profile

As mentioned above, we defined the initial conditions corresponding to a Kelvin wave in y [see (1.3)]. However, the question of more general initial transverse structure rather than a simple exponential $\exp(-y)$ is worth separate consideration.

Let us return to the equations describing the x-integrated variables $\tilde{\eta}$ and $\tilde{v}$ [see (2.9) and (2.10)]. Now the initial profile is

$$\eta|_{t=0} = \Phi(x)E(y) \qquad (5.1a)$$

or

$$\tilde{\eta}|_{t=0} = E(y)\int_{-\infty}^{\infty}\Phi(x)dx. \qquad (5.1b)$$

If we introduce

$$w = -\tilde{v}_t = \tilde{\eta} + \tilde{\eta}_y, \qquad (5.2)$$

it obeys the equation

$$w_{tt} + \gamma(w - w_{yy}) = 0, \qquad (5.3)$$

with the boundary and initial conditions

$$w|_{t=0} = E + E_y, \qquad (5.3a)$$

$$w_t|_{t=0} = 0, \qquad (5.3b)$$

$$w|_{y=0} = 0, \qquad (5.3c)$$

the first one being zero for the exponential profile. The solution for (5.3) can be written as

$$w = \int_{-\infty}^{\infty} q(l)\,\sin ly\,\cos[t\gamma^{1/2}(1 + l^2)^{1/2}]dl, \qquad (5.4)$$

where

$$q(l) = \frac{1}{\pi}\int_0^{\infty}(E + E_y)\,\cos lydy. \qquad (5.5)$$

From this integral representation it is clear that for any reasonable choice of $E(y)$, w will go to zero for large enough time. Hence we can conclude that

$$\tilde{\eta} = \int_{-\infty}^{\infty}\eta dx \to Ce^{-y}, \qquad (5.6)$$

C being some constant, and

$$\tilde{v} = \int_{-\infty}^{\infty} v dx \to 0, \qquad (5.7)$$

regardless of the initial transverse profile. The characteristic time for the adjustment is $\gamma^{-1/2}$. For much larger times, the integrals in (5.6) and (5.7) will be almost equal to their asymptotic values. That is, for long times the mass distribution in the wave tends to that of the nonlinear Kelvin wave we have just considered. The ratio of α^{-1} to $\gamma^{-1/2}$ will determine whether this happens before breaking. We also note that $E(y)$ itself cannot be chosen arbitrarily since the no-flow condition at the coast requires that it behave like $\exp(-y)$ for small y. These factors lead to a similar wave evolution for different initial profiles in y.

We conducted a number of numerical experiments, that confirming waves with different initial transverse structure developed similar features, including breaking over the uniform phase zone. Figure 12 reveals some differences in the evolution of the amplitude at the coast for the initial transverse structure $\sim e^{-2y}$, $\sim e^{-y/2}$, and $\sim e^{-y}$ ($\alpha = 0.125$, $\gamma = 0.5$). In the first two cases the initial adjustment time is given accurately by $\gamma^{-1/2}$. Then the amplitudes slowly decay with time.

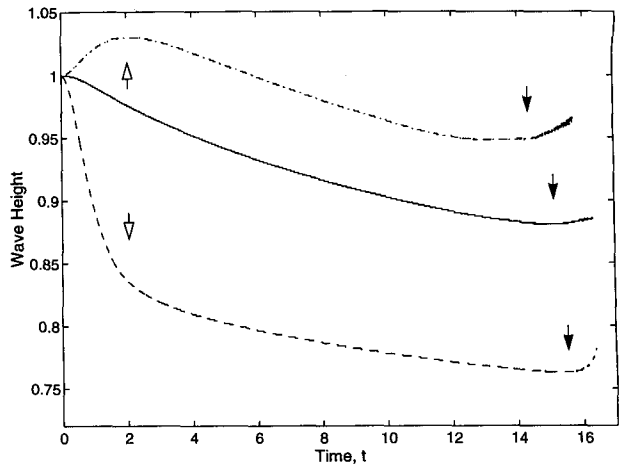

FIG. 12. The evolution of the amplitude at the coast for three different initial transverse structures with slopes $\sim e^{-y/2}$, e^{-y}, and $\sim e^{-2y}$, starting from the top plot. For the first and the third cases the adjustment time is given accurately by $\gamma^{-1/2}$ and is shown by open arrows. The irregularities at the end of the plots indicated by filled arrows correspond to breaking; for $\alpha = 0.125$, $\gamma = 0.5$.

The wave with the faster initial transverse decay experiences a stronger decrease in amplitude, while the characteristic lengths do not change. This effectively decreases the nonlinearity for such waves, which makes them more stable and longer lived.

6. Conclusions

From the above discussion we can conclude that nonlinear nondispersive Kelvin waves may display some features that are independent of the details of the analytical model. The delay of breaking, if it occurs, and the establishment of a zone of uniform phase adjacent to the coast are among such features that depend on the combined action of rotation and transverse effects. As in the corresponding linear problem, the influence of the coastal boundary is felt to distances comparable to the Rossby radius but is now extended to include the nonlinear phenomenon of breaking.

The delay in breaking and the establishment of the uniform phase zone is related to the transverse mass flux associated with the jetlike flow at the front of the wave. Moving away from the coast, the offshore velocity increases at first, corresponding to an offshore flux. After reaching its maximum, it decreases monotonically, corresponding to a deposition of mass offshore. On the longer timescales this leads to a uniform speed of the wave front, since increasing steepness leads to a greater offshore flux from regions of larger to smaller nonlinearity. We see from both the numerical and analytical solutions that this mass flux leads to the uniform phase zone and breaking almost simultaneously across the zone. To the extent that the numerical solutions resolve it, the approach to breaking is typical

of long nonlinear waves in hyperbolic systems. The onset of breaking is determined by the evolution of the wave phase and appears to be independent of the local wave amplitude, which varies with distance from the boundary.

As with models of long nonlinear waves in nonrotating systems, in the absence of dispersion all waves of finite mass break, while dispersion suppresses breaking (Whitham 1974). We expect that in nature whether or not hyperbolic breaking occurs will depend not only on the presence of dispersion but also on the effects of viscosity and background turbulence leading to the dissipation of the wave energy. In addition, other hydrodynamic instabilities (e.g., Kelvin–Helmholtz) may set in prior to breaking, leading to wave-generated turbulence and dissipation. In the absence of dissipation we have made estimates of the time and distance to breaking for an internal Kelvin wave of 10-m amplitude, 5-km length, and characteristic period 1.5 h, for a Rossby radius of 10 km (appendix A). For these parameters we expect the distance and time to breaking to be about 80 km and 21 hours, respectively.

In another example, a Kelvin wave of 50-m amplitude, 50-km length, propagating in the marine atmospheric layer adjacent to the Californian coast (height 500 m, Rossby radius of 150 km—from Hermann et al. 1990) will have a characteristic period of about 1 h. This gives the distance and time to breaking as 750 km and 14 hours.

Acknowledgments. This work was supported by a grant from the Office of Naval Research, Coastal Sciences. We are also grateful to the anonymous referees for several helpful comments on the original paper.

APPENDIX A

Estimates of Parameters in the Evolution Equations

A detailed derivation of coupled evolution equations for long nonlinear internal waves in a two-layer fluid is given by Tomasson (1991) (see also Renouard et al. 1992). These equations include three-dimensional, rotational, and dispersive effects:

$$\eta_t + \eta_x + \alpha\eta\eta_x + \beta\eta_{xxx} + \gamma(v_y - v) = 0 \quad \text{(A.1)}$$

$$v_t + \eta_y + \eta = 0. \quad \text{(A.2)}$$

This set of equations is asymptotically equivalent to the modified Kadomtsev–Petviashvili (KP) equation (Grimshaw and Melville 1989), which can be obtained by assuming that $v_t \approx -v_x$, and cancelling v from (A.1) and (A.2).

From Tomasson (1991) the expressions for α, β, and γ are

$$\alpha = \frac{3h}{2H} \quad \text{(A.3a)}$$

$$\beta = \frac{1}{2}\left(\frac{H}{L}\right)^2 \quad \text{(A.3b)}$$

$$\gamma = \frac{1}{2}\left(\frac{L_x}{\mathrm{Ro}}\right)^2, \quad \text{(A.3c)}$$

where h is a typical wave amplitude, L_x is a typical wavelength, H is an equivalent depth of the interface, and Ro is the Rossby radius of deformation. If f is the Coriolis parameter, c is the linear phase speed of the waves, g is the acceleration of gravity, and $\Delta\rho/\rho$ is a relative change of the density on the interface, then

$$c = \left(\frac{\Delta\rho}{\rho} gH\right)^{1/2} \quad \text{and} \quad \mathrm{Ro} = \frac{c}{f}. \quad \text{(A.4)}$$

We choose the following values for an oceanic Kelvin wave:

$$\Delta\rho/\rho = 10^{-3}, \quad H = 100 \text{ m},$$

$$h = 10 \text{ m}, \quad L_x = 5 \text{ km}.$$

For these values $c = 1 \text{ m s}^{-1}$, Ro = 10 km, with

$$\alpha = 0.15, \quad \gamma = 0.125, \quad \text{and} \quad \beta = 0.67 \times 10^{-4}.$$

The above example confirms that the dispersion for such a Kelvin wave may be very small with respect to the rotational and nonlinear effects, and we can neglect the dispersion for a rather large range of wavelengths. So for the values of H and $\Delta\rho/\rho$ selected, one may apply our basic system; that is, $\alpha \sim \gamma$ and $\beta \ll \alpha$ if, roughly, 3 km $\leq L_x \leq$ 10 km, or if the wave period is between 1 and 3 hours. Nevertheless, the smallness of β for larger scales does not rule out the possibility that, when the wave is steepening, local dispersion may arise as an important factor in determining the detailed character of the breaking itself. Also notice that the derivation of the equations requires that α, β, and γ be much smaller than 1. This implies $L \ll$ Ro. However, even for $L_x = 1/2$ Ro, $\gamma = 0.12$ is already much less than 1. Therefore, we may relax this condition and require only $L_x <$ Ro, which should still ensure acceptable accuracy.

APPENDIX B

Lagrangian Formulation for the Analytical Model

The application of the average-Lagrangian technique (Whitham 1974) is nontraditional for hyperbolic or quasihyperbolic systems. Usually it is used for the description of the linear or nonlinear waves in dispersive media (Fedorov and Malomed 1992). However, we believe that it can be applied to hyperbolic waves as well.

It can be shown that the Lagrangian for the system (2.1) and (2.2) is

$$L = \frac{1}{2}\phi_x\phi_t + \frac{\alpha}{6}(\phi_x)^3 + \gamma\psi_x\left(\frac{\psi_t}{2} - \frac{\psi_x}{2} + \phi_y + \phi\right), \quad \text{(B.1)}$$

where ϕ, ψ are potential functions and $\eta = \phi_x$, $v = \psi_x$. It can also be written as

$$L = \frac{1}{2}\eta\phi_t + \frac{\alpha}{6}\eta^3 + \gamma\frac{v}{2}(\psi_t - v) + \gamma\psi_x(\phi_y + \phi). \tag{B.2}$$

Now we integrate the expressions (4.6) through (4.8) for η and v to obtain

$$\phi = \Re + \Theta\frac{\Phi^2}{2}, \tag{B.3}$$

$$\phi_t = \frac{a_t}{a}e^{-y}\Phi\xi + \left(2\frac{a_t}{a}\Theta - \Theta_t\right)e^{-y}\frac{\Phi^2}{2}, \tag{B.4}$$

$$\phi_y + \phi = \frac{a_y}{a}e^{-y}\Phi\xi + \left(2\frac{a_y}{a}\Theta - \Theta_y\right)e^{-y}\frac{\Phi^2}{2}, \tag{B.5}$$

$$\psi = be^{-y}\frac{\Phi^2}{2} + de^{-y}\Phi\xi, \tag{B.6}$$

where

$$\Re = \Re(\xi) = \int \Phi(\xi)d\xi. \tag{B.7}$$

Introducing

$$\tilde{\Theta} = \frac{\Theta}{a^2} \tag{B.8}$$

reduces (B.4) and (B.5) to

$$\phi_t = \frac{a_t}{a}e^{-y}\Phi\xi - a^2\tilde{\Theta}_t e^{-y}\frac{\Phi^2}{2} \tag{B.9}$$

and

$$\phi_y + \phi = \frac{a_y}{a}e^{-y}\Phi\xi - a^2\tilde{\Theta}_y e^{-y}\frac{\Phi^2}{2}. \tag{B.10}$$

Substituting into the Lagrangian, integrating over x, and making several transformations gives the averaged Lagrangian (with higher-order terms omitted)

$$\tilde{L} = \frac{Ie^{-2y}}{3}\left[-\frac{1}{2}a^2\Theta_t + \frac{\alpha}{2}a^2e^{-y} + \frac{\gamma}{2}(db_t - bd_t)\right.$$

$$\left. - \frac{\gamma}{2}\tilde{q}b^2 - \frac{\gamma}{2}\tilde{r}d^2 - \gamma da^2\Theta_y - \gamma b\frac{a_y}{a}\right]. \tag{B.11}$$

Applying the Eulerian variational principle to $\tilde{L}$ successively with respect to a, $\tilde{\Theta}$, d, and b, we obtain a set of equations similar to those derived before, with $\tilde{r}$, $\tilde{q}$ in place of r and q:

$$a^2\tilde{\Theta}_t + \gamma(2b - b_y) = \alpha a^2e^{-y}$$

$$-\frac{a_t}{a} + \gamma(2d - d_y) = 0$$

$$b_t - a^2\tilde{\Theta}_y - \tilde{r}d = 0$$

$$d_t + \frac{a_y}{a} + \tilde{q}b = 0. \tag{B.12}$$

The expressions for $\tilde{r}$, $\tilde{q}$, and I are

$$\tilde{r} = \frac{3}{I}\int_{-\infty}^{\infty}\Phi^2\Phi_x^2dx;$$

$$\tilde{q} = \frac{3}{I}\int_{-\infty}^{\infty}(\Phi\xi)_x^2dx; \quad I = \int_{-\infty}^{\infty}\Phi^3dx. \tag{B.13}$$

In principle, $\tilde{r}$ and $\tilde{q}$ depend on Θ and, consequently, on t and y. To obtain simpler linear equations we should replace them with some constant effective values. An advantage of this approach is that regardless of particular functions in the expansion for v, the final equations (B.12) will be unchanged, while the coefficients $\tilde{r}$, $\tilde{q}$ will be modified. This proves to be a rather universal character of the system.

REFERENCES

Baines, P. G., 1980: The dynamics of the southerly buster. *Aust. Meteor. Mag.*, **28,** 175–200.

Bannon, P. R., 1981: Synoptic scale forcing of coastal flows: Forced double Kelvin waves in the atmosphere. *Quart. J. Roy. Meteor. Soc.*, **107,** 313–327.

Beardsley, R. C., C. E. Dorman, C. A. Friehe, L. K. Rosenfeld, and C. D. Winant, 1987: Local atmospheric forcing during the CODE. Part 1: A description of the marine boundary layer and atmospheric conditions over a northern California upwelling region. *J. Geophys. Res.*, **92,** 1467–1488.

Bennet, J. R., 1973: A theory of large-amplitude Kelvin waves. *J. Phys. Oceanogr.*, **3,** 57–60.

Boyd, J. P., 1980: The nonlinear equatorial Kelvin wave. *J. Phys. Oceanogr.*, **10,** 1–11.

Dorman, C. E., 1985: Evidence of Kelvin waves in california's marine layer and related eddy generation. *Mon. Wea. Rev.*, **113,** 827–839.

Fedorov, A. V., and B. A. Malomed, 1992: Generation of flexural waves on a quasi-one-dimensional KP soliton. *Wave Motion,* **15,** 221–227.

Gill, A. E., 1977: Coastally trapped waves in the atmosphere. *Quart. J. Roy. Meteor. Soc.*, **103,** 431–440.

Grimshaw, R., 1985: Evolution equations for weakly nonlinear, long internal waves in a rotating fluid. *Stud. Appl. Math.*, **73,** 1–33.

——, and W. K. Melville, 1989: On the derivation of the modified Kadomtsev–Petviashvili equation. *Stud. Appl. Math.*, **80,** 183–202.

Hermann, A. J., B. M. Hickey, C. F. Mass, and M. D. Albright, 1990: Orographically trapped coastal wind events in the Pacific Northwest and their oceanic response. *J. Geophys. Res.*, **95**(c8), 13 169–13 193.

Hsieh, W. W., M. K. Daley, and R. C. Wajsowitcz, 1983: The free Kelvin wave in finite-difference numerical models. *J. Phys. Oceanogr.*, **13,** 1383–1397.

Hua, B., and F. Thomasset, 1983: A numerical study of the effects of coastline geometry on wind-induced upwelling in the Gulf of Lions. *J. Phys. Oceanogr.*, **13,** 678–694.

Katsis, C., and T. R. Akylas, 1987: Solitary internal waves in a rotating channel: A numerical study. *Phys. Fluids,* **30,** 297–301.

Macomb, E. S., 1986: The interaction of nonlinear waves and currents with coastal topography. M.S. thesis, Dept. of Civil Engineering, Massachusetts Institute of Technology.

Mark, J. R., 1974: Acoustic Radar Investigations of Boundary Layer Phenomena. Rep. NAS8-28659. Dept. of Meteorology, University of Oklahoma.

Maxworthy, T., 1983: Experiments on solitary internal Kelvin waves. *J. Fluid Mech.,* **129,** 356–383.

Melville, W. K., G. G. Tomasson, and D. P. Renouard, 1989: On the stability of Kelvin waves. *J. Fluid Mech.,* **206,** 1–23.

——, D. P. Renouard, and X. Zhang, 1990: On the generation of nonlinear internal Kelvin waves in a rotating channel. *J. Geophys. Res.,* **95**(C10), 18 247–18 254.

Pedlosky, J., 1987: *Geophysical Fluid Dynamics.* Springer-Verlag.

Renouard, D. P., G. Chabert D'Hires, and X. Zhang, 1987: An experimental study of strongly nonlinear waves in rotating system. *J. Fluid Mech.,* **177,** 381–394.

——, G. G. Tomasson, and W. K. Melville, 1992: An experimental and numerical study of nonlinear internal waves. *Phys. Fluids A,* **5,** 1401–1411.

Smith, R. K., N. Crook, and G. Roff, 1982: The morning glory: An extraordinary atmospheric undular bore. *Quart. J. Roy. Meteor. Soc.,* **108,** 937–956.

Tomasson, G. G., 1991: Nonlinear waves in a channel: Three-dimensional and rotational effects. Ph.D. thesis, Dept. of Civil Engineering, Massachusetts Institute of Technology.

——, and W. K. Melville, 1990: Nonlinear and dispersive effects in Kelvin waves. *Phys. Fluids A,* **2**(2), 189–193.

——, and ——, 1992: Geostrophic adjustment in a channel: Nonlinear and dispersive effects. *J. Fluid Mech.,* **241,** 23–57.

Whitham, G. B., 1974: *Linear and Nonlinear Waves.* Wiley.